Proposal # PR-00-004 **Hall:** C

Title: Duality in Meson Electroproduction

Contact person: Chris Armstrong (JLab)

Beam time request:

Days requested for approval:	15
Tune up time included in request:	yes

Beam characteristics:

Energy:	6.0GeV
Current:	50 μA
Polarization:	no

Targets:

Nuclei:	LH_2, LD_2 Al (MT)
Rastering:	nominal
Polarized:	no

Spectrometers:

HMS	single arm mode
SOS	luminosity monitor

Special requirements/requests:

Low profile pipe to beam dump to allow HMS operation at 10.5° (as configured during E93-021).

Possible fabrication and installation of an aerogel Cherenkov detector in the HMS.

Proposal # PR-00-004 **Hall:** C

Title: Duality in Meson Electroproduction

Contact person: Chris Armstrong (JLab)

Theoretical comments:

1. The successful pQCD explanation of the hard processes such as diffractive electroproduction of mesons is based on factorization. Since there is no quantitative theory of higher-twist effects we do not know at which Q^2 (if any) factorization fails. The proposed experiment will check whether factorization does hold at moderate energies and Q^2~ few GeV^2. In addition, it will check quark-hadron duality for this kinematical region. The results of the experiment will also enrich our knowledge of higher-twist effects which are an important source of information about the structure of the nucleon.

Technical comments:

1. This experiment needs to run the HMS angle as low as 10.5°, so there may be some setup time involving installation of the downstream pipe and certification of the spectrometer angle range.

2. In order to separate pions from heavier hadrons they propose pressurizing the HMS gas cerenkov to 1.4 atm. This will be essential for future HMS-SHMS operations and would represent a valuable improvement to Hall C capabilities. The first time this is done the HMS cerenkov must be removed from the detector hut, the windows changed, certified to 1.4 atm. The tank would then be reinstalled in the detector hut, and filled with C4F10. This whole process could take several weeks and would best be done during a long downtime. Converting the gas cerenkov back to sub-atmospheric for other experiments will also take a few days, and again would best be done during a long downtime. C4F10 condenses at room temperature at a surprisingly low over-pressure. The collaboration should look up the data tables and be prepared to show that it is not a problem.

3. The collaboration says that they MIGHT put an aerogel in HMS in order to separate protons from lighter hadrons (and so, in conjunction with the gas cerenkov, to positively identify kaons). That would be another important new capability on the way to HMS-SHMS operations at higher energies. They would need an aerogel with an index of something like 1.04 for this experiment which is probably buildable. At a minimum it would probably require cutting the exit pipe, moving the Wire Chambers's forward, and installing the aerogel before the first hodoscope. That would require a major down-time, as significant effort to prepare new mounting hardware/flanges and a complete survey of the detector package. In addition, approximately 1/2 week of beam time and one month of analysis will likely be required to get the optics back after moving the wire chambers.

JLAB USER GROUP

Jefferson Lab PAC16
Proposal Cover Sheet

This document must be received by close of business Thursday,

June 8, 1998t:

Jefferson Lab
User Liaison,
Mail Stop 12B
12000 Jefferson Ave.
Newport News, VA
23606

Experimental Hall: C

Days Requested for Approval: 15

❒ Proposal Title:

Duality in Meson Electroproduction

Proposal Physics Goals

Indicate any experiments that have physics goals similar to those in your propos

Approved, Conditionally Approved, and/or Deferred Experiment(s) or proposals:

None

Contact Person

Name: CHRIS ARMSTRONG
Institution: JEFFERSON LAB
Address: 12000 JEFFERSON AVE
Address: MS 12H
City, State, ZIP/Country: NEWPORT NEWS, VA 23606 USA
Phone: 757-269-7168 Fax: 757-269-5235
E-Mail: csa@jlab.org

Jefferson Lab Use On

Receipt Date: 12/14/99 PR-00-004

By: S. Cannella

HAZARD IDENTIFICATION CHECKLIST

JLab Proposal No.: _____ Date: _____

(For CEBAF User Liaison Office use only.)

Check all items for which there is an anticipated need.

Cryogenics
- _____ beamline magnets
- _____ analysis magnets
- _____ target
  - type: _____
  - flow rate: _____
  - capacity: _____

Electrical Equipment
- _____ cryo/electrical devices
- _____ capacitor banks
- _____ high voltage
- _____ exposed equipment

Radioactive/Hazardous Materials

List any radioactive or hazadorous/ toxic materials planned for use:

_____

_____

_____

_____

Pressure Vessels
- _____ inside diameter
- _____ operating pressure
- _____ window material
- _____ window thickness

Flammable Gas or Liquids
- type: _____
- flow rate: _____
- capacity: _____

Drift Chambers
- type: _____
- flow rate: _____
- capacity: _____

Other Target Materials
- ___ Beryllium (Be)
- ___ Lithium (Li)
- ___ Mercury (Hg)
- ___ Lead (Pb)
- ___ Tungsten (W)
- ___ Uranium (U)
- ___ Other (list below)

_____

_____

Vacuum Vessels
- _____ inside diameter
- _____ operating pressure
- _____ window material
- _____ window thickness

Radioactive Sources
- _____ permanent installation
- _____ temporary use
- type: _____
- strength: _____

Large Mech. Structure/System
- _____ lifting devices
- _____ motion controllers
- _____ scaffolding or
- _____ elevated platforms

Lasers
- type: _____
- wattage: _____
- class: _____

Installation:
- _____ permanent
- _____ temporary

Use:
- _____ calibration
- _____ alignment

Hazardous Materials
- ____ cyanide plating materials
- ____ scintillation oil (from)
- ____ PCBs
- ____ methane
- ____ TMAE
- ____ TEA
- ____ photographic developers
- ____ other (list below)

_____

_____

General:

Experiment Class:
- _____ Base Equipment
- _____ Temp. Mod. to Base Equip.
- _____ Permanent Mod. to Base Equipment
- _____ Major New Apparatus

Other: _____

_____

Standard Hall C equipment only

BEAM REQUIREMENTS LIST

Lab Proposal No.: _____ Date: _____

Hall: C Anticipated Run Date: _____ PAC Approved Days: _____

Spokesperson: CHRIS ARMSTRONG Hall Liaison: Rolf Ent
Phone: 757-269-7168
E-mail: csa@jlab.org

List all combinations of anticipated targets and beam conditions required to execute the experiment. (This list will form the primary basis for the Radiation Safety Assesment Document (RSAD) calculations that must be performed for each experiment.)

Condition No.	Beam Energy (MeV)	Mean Beam Current (μA)	Polarization and Other Special Requirements (e.g., time structure)	Target Material (use multiple rows for complex targets — e.g., w/windows)	Material Thickness (mg/cm²)	Est. Beam-On Time for Cond. No. (hours)
1	6000	50	None	LH2	0.29	140
				Al	0.11	140
2	6000	50		LD2	0.65	140
				Al	0.11	140
3	6000	30		Al	0.50	18

The beam energies, E_{Beam}, available are: $E_{Beam} = N \times E_{Linac}$ where N = 1, 2, 3, 4, or 5. E_{Linac} = 800 MeV, i.e., available E_{Beam} are 800, 1600, 2400, 3200, and 4000 MeV. Other energies should be arranged with the Hall Leader before listing.

LAB RESOURCES LIST

JLab Proposal No.: _____ Date _____

(For JLab ULO use only.)

List below significant resources — both equipment and human — that you are requesting from Jefferson Lab in support of mounting and executing the proposed experiment. Do not include items that will be routinely supplied to all running experiments such as the base equipment for the hall and technical support for routine operation, installation, and maintenance.

Major Installations *(either your equip. or new equip. requested from JLab)*

_____

_____

_____

_____

_____

New Support Structures: _____

_____

_____

_____

Data Acquisition/Reduction

Computing Resources: _____

_____

_____

_____

New Software: _____

_____

_____

_____

Major Equipment

Magnets: _____

_____

Power Supplies: _____

_____

Targets: _____

_____

Detectors: We are considering installation of ~~an~~ an aerogel $\check{C}$ detector in HMS; if so, we'd need Hall C help for installation and instrumentation.

Electronics: _____

_____

Computer Hardware: _____

_____

Other: _____

_____

Other: Reinstallation of low-profile pipe to beam dump for operation of HMS at 10.5°

_____

_____

_____

Computing Requirements for Duality in Meson Electroproduction

C. Armstrong
December 14, 1999

- Raw Data: ≈500 GB.
- Computer resources for reconstruction and analysis: ≈30,000 SPECint95 hours.
- Computer resources for simulations: ≈30,000 SPECint95 hours.
- On-line disk space: ≈100 GB.
- No foreseen need to transfer data to other institutions.
- No other special requirements.

Duality in Meson Electroproduction

December 14, 1999

Submitted by

C. S. Armstrong (spokesperson), R. Ent, J. Mitchell
Jefferson Laboratory, Newport News, VA

H. Mkrtchyan (spokesperson), R. Asaturyan, S. Stepanyan, V. Tadevosyan
Yerevan Physics Institute, Armenia

D. Meekins
Florida State University, Tallahassee, FL

I. Niculescu
George Washington University, Washington, DC

H. Bitao, M. E. Christy, A. Cochran, C. Jackson, C. E. Keppel
Hampton University, Hampton, VA

P. Stoler
Rensselaer Polytechnic Institute, Troy, NY

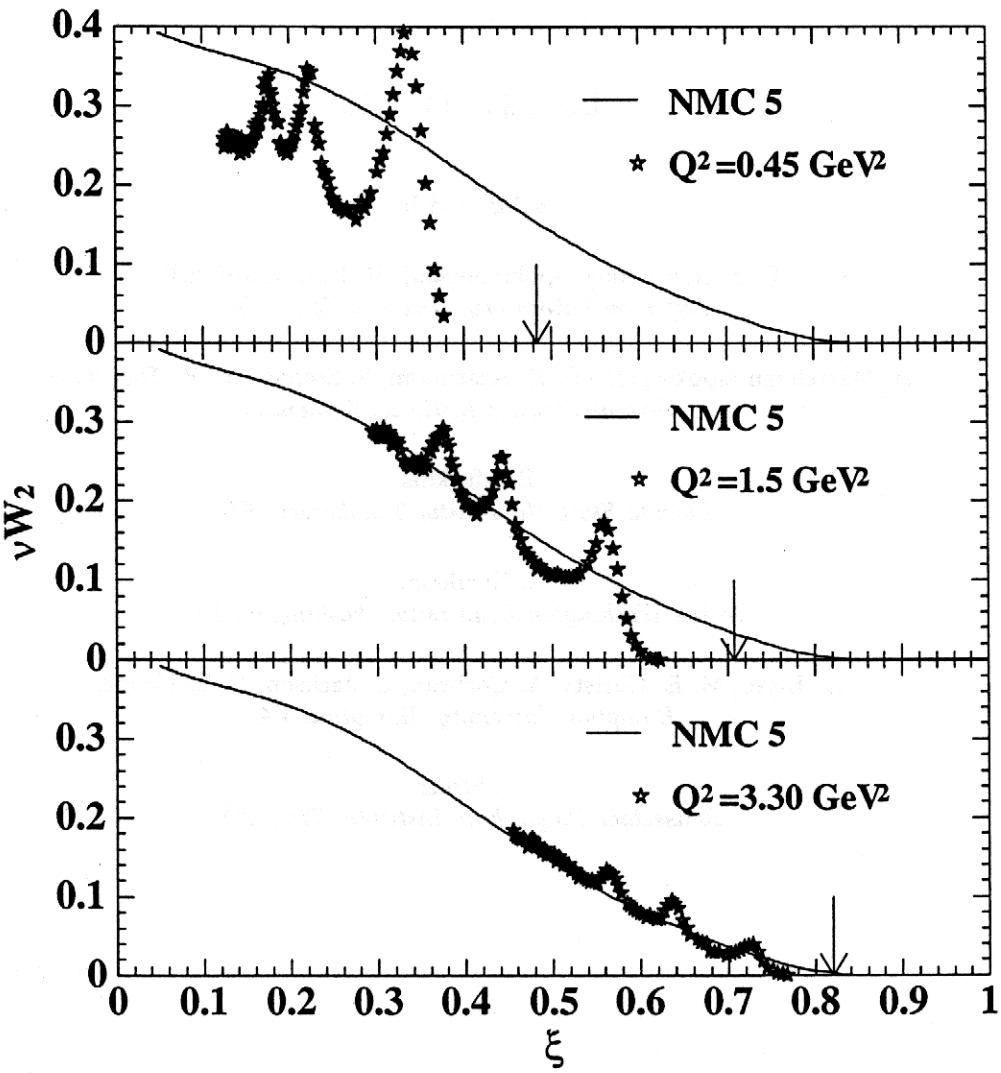

Figure 1: νW_2 versus ξ for Jefferson Lab resonance data [Nic98] at three different values of Q^2 (the variable ξ may be treated as Bjorken x modified to account for target mass effects). The data are (e, e') scans in the resonance region, corrected to the central value of Q^2 indicated (arrows indicate the position of the elastic peak). The lines show the NMC parameterization [Arn95] at $Q^2 = 5$ (GeV/c)^2.

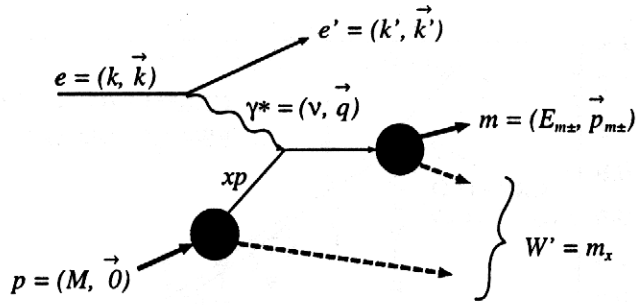

Figure 2: A diagram of meson electroproduction. In the proposed experiment, we detect the outgoing electron e and the outgoing meson m (a charged pion or kaon).

of this proposal is to explore the extent to which the electroproduction of mesons exhibits this same dual behavior between resonance region scattering and DIS. In analogy with the inclusive case, Carlson suggests several phenomena one could look for by 'tagging' a meson in the final state [Car98]:

- Do we observe scaling behavior as Q^2 increases?
- Do the resonances tend to fall along the DIS scaling curve?
- Does the ratio of resonant to non-resonant strength remain constant as we change Q^2? It could be that the anomalously rapid fall of the Δ resonance with momentum transfer observed in some channels is 'accidental' and that we might not see the same behavior in meson-tagged measurements.[1]

Fig. 2 shows a diagrammatic figure of meson electroproduction. For reasons that will be explained below, we treat the interaction at lowest order as knockout of a quark and subsequent (independent) hadronization. The struck quark carries momentum xp, where x is the fraction of the light-cone momentum of the target nucleon carried away by the struck quark.[2] The outgoing meson is detected (as is the outgoing electron), and we define z in terms of target, photon, and meson four vectors: $z = (p \cdot m)/(p \cdot \gamma^*)$. In the target rest (lab) frame, this becomes $z = E_m/\nu$, the fraction of the virtual photon energy taken away by the meson. In the elastic limit, $z = 1$, and the meson carries away all of the photon's energy. We define $p_\perp$ to be the transverse momentum of the meson in the virtual photon-nucleon system.

We reconstruct the invariant mass m_x that goes undetected. Here we refer to this quantity as W' to highlight the fact that *it could play a role analogous to W for duality in the inclusive case.* If we neglect the meson mass, W'^2 is given by

$$W'^2 = W^2 - 2z\nu\,(m_p + \nu - |\vec{q}|\cos\theta_{qm})\,,$$

where $\nu = E - E'$ and θ_{qm} is the lab angle between the virtual photon momentum $|\vec{q}|$ and the outgoing meson momentum $|\vec{p}|$. As in the usual inclusive scattering case, the square of the (inclusive) invariant mass W is given by

$$W^2 = m_p^2 + Q^2\,(\frac{1}{x} - 1)\,.$$

[1] In particular, the fall of the Δ resonance may be the result of accidental cancellation of terms that contribute to $G_+(Q^2)$. It may be that measurements in different channels are not subject to the same cancellation and do not observe this rapid fall.

[2] For our purposes we take x to be Bjorken x, but ultimately it should contain appropriate modifications.

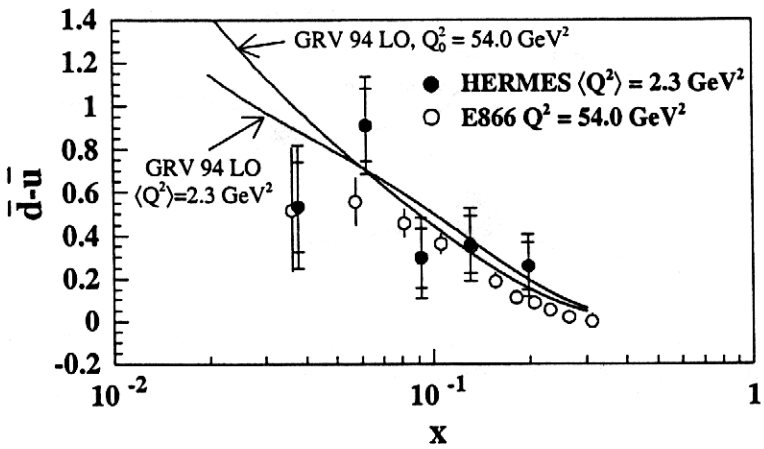

Figure 4: $\overline{d} - \overline{u}$ as a function of x at both moderate and high energy loss.

E GeV	$\theta_{e'}$ deg.	E' GeV	Q^2 $(\mathrm{GeV}/c)^2$	x	θ_π deg.	p_π GeV/c	z	W'^2 GeV^2
5.51	30.0	1.6	2.36	0.32	13.0	2.0	0.51	3.3
						2.5	0.64	2.6
						3.0	0.77	2.0

Table 1: Central kinematics for the 1999 Jefferson Lab test runs.

Evidence of factorization in meson electroproduction at even lower energies is apparent in the results of several test runs made in Hall C of Jefferson Lab in August 1999. The data included measurements of semi-inclusive pion electroproduction, $(e, e'\pi^\pm)X$, on ^{1}H, ^{2}H, and Al at low energy [$\nu = 3.9$ GeV, $W^2 = 5.9$ GeV^2, $Q^2 = 2.4$ (GeV/c)^2]. The kinematics, which are similar to those proposed for this experiment, are given in Table 1. A coincidence time spectrum for one of the runs, showing the easily separable pion peak, is given in Fig. 5. We assume that factorization holds, as in Eq. 2, which allows us to extract the fragmentation functions $D_{q_i}^{\pi^\pm}(z)$ from the data. Fig. 6 shows the results, plotted as a function of z. The solid line is a next-to-leading order (NLO) fragmentation function fit to e^+e^- data at high energy ($s = W^2 = 840$ GeV^2) [Bin95] and evaluated at the momentum transfer of our data. The agreement between the data and the NLO curve suggests that *factorization is working quite well in this kinematic regime.*

Using the Jefferson Lab test data on both hydrogen and deuterium, we can extract the ratio of probability distributions for finding down to up valence quarks in the nucleon, d_v/u_v. We assume charge conjugation invariance, isospin symmetry and a charge ratio of valence quarks $q_u^2/q_d^2 = 4$, which allows us to use charged pion yields on both targets to extract d_v/u_v. The procedure, which follows that found in Ref. [Mar77], assumes factorization. The single Jefferson Lab point is plotted in Fig. 7 together with a collection of data from neutrino measurements at hundreds of GeV (CDHS, WA 21/25) [Glu98, and references therein]. Here, again, *the agreement between experiments from very low to very high energy loss strongly suggests that factorization holds well down to low energy losses.*

The behavior witnessed in the above examples is quite remarkable, although all of it would be consistent with dual behavior in meson electroproduction between the resonance and DIS regions. Regardless, in this experiment we will investigate whether the factorization approach is valid at relatively low energy loss ν but large W'^2 (> 3 GeV^2) by trying to extract the fragmentation functions $D^{\pi\pm}(z)$ from this data and verifying the $p_\perp$ dependence. In particular, are the extracted fragmentation functions and associated $p_\perp$

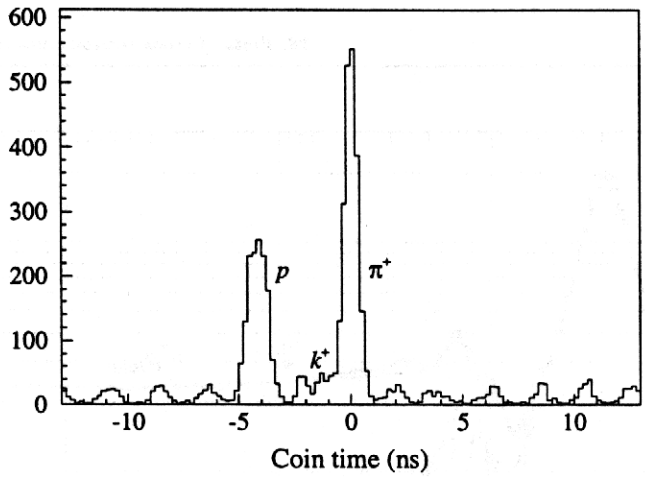

Figure 5: A coincidence time spectrum from one of the positive polarity Jefferson Lab test runs, showing clear peaks at 0 ns (π^+) and at -4 ns (protons). There is a small kaon peak (just visible) at -1 ns. The 2 ns RF structure of the electron beam is visible in the multiple accidental peaks.

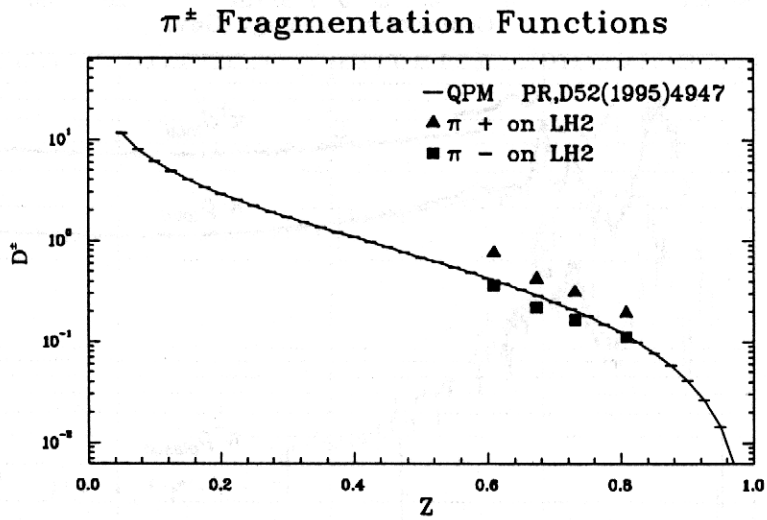

Figure 6: A comparison between $\pi^\pm$ electroproduction data at low energy (triangles and squares) and a next-to-leading order (NLO) fragmentation function fit to high energy data (solid line). The curve corresponds to the average of positive and negative fragmentation functions, which should be compared to the average of each pair of $\pi^\pm$ data points. The data shown here were limited to pion momenta above 2.4 GeV/c in order to avoid $\pi^\pm N$ interactions in the final state.

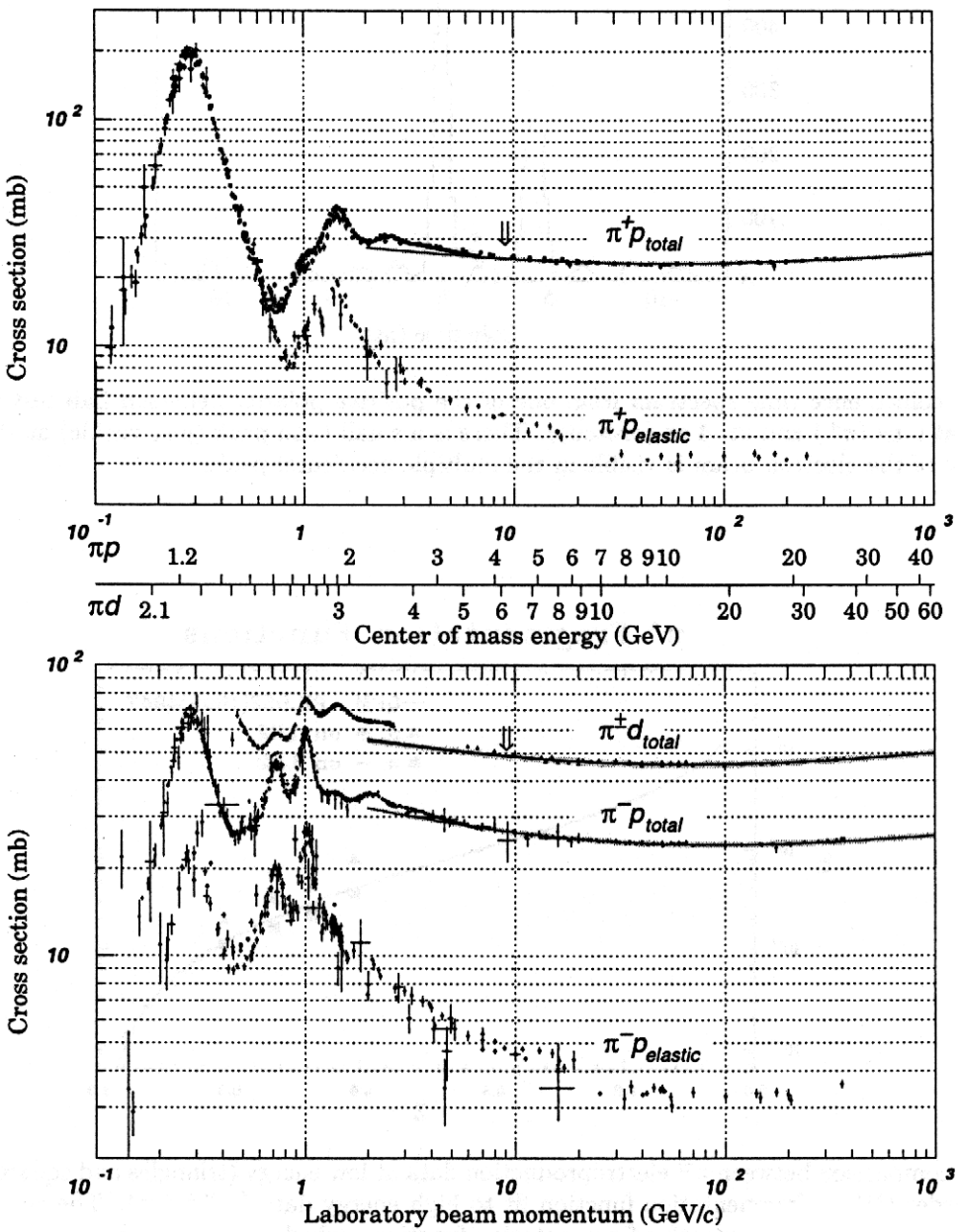

Figure 38.20: Total and elastic cross sections for $\pi^\pm p$ and $\pi^\pm d$ (total only) collisions as a function of laboratory beam momentum and total center-of-mass energy. Corresponding computer-readable data files may be found at `http://pdg.lbl.gov/xsect/contents.html` (Courtesy of the COMPAS Group, IHEP, Protvino, Russia, April 1998.)

Figure 8: A plot from the Particle Data Group showing $\pi^\pm p$ and $\pi^\pm d$ cross sections.

techniques we can use to reduce our dependence on Monte Carlo simulation.[5] The first technique uses the simultaneously measured inclusive cross section $\frac{d\sigma}{d\Omega_e dE_e}$ to eliminate the need for a Monte Carlo simulation of the electron spectrometer, and the second uses the small acceptance of the meson spectrometer to allow an analytical integration over $p_\perp$, eliminating the need for a full simulation of the meson spectrometer.

The meson yield $\frac{dN}{dz}$ conventionally arises in terms of a fit (with parameters b, A, and B) to the cross section [Dak73, Eq. 3], with normalization provided by the corresponding inclusive cross section:

$$\frac{\frac{d\sigma}{d\Omega_e dE_e dx dp_\perp^2 d\phi}}{\frac{d\sigma}{d\Omega_e dE_e}} = \frac{dN}{dz}\, b \exp(-bp_\perp^2)\, \frac{1 + A\cos(\phi) + B\cos(2\phi)}{2\pi}. \tag{3}$$

We use the relationships $d\Omega_m dp_m = \frac{1}{2p_m^2}\, dp_\perp^2\, dp_\parallel\, d\phi$ and $dp_\parallel = \nu dx$ to rewrite Eq. 3 as

$$\frac{\frac{d\sigma}{d\Omega_e dE_e d\Omega_m dp_m}}{\frac{d\sigma}{d\Omega_e dE_e}} = \frac{2p_m^2}{\nu}\, \frac{dN}{dz}\, b \exp(-bp_\perp^2)\, \frac{1 + A\cos(\phi) + B\cos(2\phi)}{2\pi}. \tag{4}$$

There is no evidence of a ϕ dependence [Dak73], and where possible we position the meson spectrometer along the direction of momentum transfer, effectively integrating over ϕ:

$$\frac{\frac{d\sigma}{d\Omega_e dE_e d\Omega_m dp_m}}{\frac{d\sigma}{d\Omega_e dE_e}} = \frac{2p_m^2}{\nu}\, \frac{dN}{dz}\, b \exp(-bp_\perp^2). \tag{5}$$

We now take advantage of the small $p_\perp$ acceptance of the apparatus by expanding $\exp(-bp_\perp^2)$ and performing an analytical integration from 0 to $p_{\perp max}$ (the latter can be obtained to good accuracy from geometrical arguments or from a very simple Monte Carlo simulation). The parameter b, which we will extract from our data, is also available from fits to other data [Dak73]. The result is an expression of the meson yield in terms of the measured inclusive and coincidence cross sections:

$$\frac{dN}{dz} = \frac{1}{2\pi b p_{\perp max}^2}\, \frac{\frac{d\sigma}{d\Omega_e dE_e d\Omega_m dp_m}}{\frac{d\sigma}{d\Omega_e dE_e}}. \tag{6}$$

Expected Rates and Background Estimates

Pion coincidence event rates for this experiment (assuming 50 μA beam current) are of order 1 Hz (estimate based on the Hall C test runs), with kaon rates down from that by factors of roughly ten to one hundred. Our goal is to collect statistics that will result in 1–2% uncertainties in the pion yield per hadron setting, which corresponds to about two hours per setting. The systematic uncertainty will in all cases be as large or larger than these statistical uncertainties. As we do not have complete $p_\perp$ and ϕ coverage, we need to assume $p_\perp$ and ϕ dependences of the cross section beyond our acceptances (in particular to estimate the effect of radiative processes). We believe a systematic uncertainty of 5 to 10% is achievable and sufficient for this initial test. Based on the test runs we also estimate that worst-case accidental coincidences will result in a signal-to-noise ratio in the coincidence peak of approximately 4:1.

Table 3 gives the beam time requested for the experiment. When estimating time for configuration changes, we assumed 10 minutes per target change, 25 minutes per HMS or SOS momentum change, and 2 hours for a single HMS polarity change.

[5] We plan to perform the final analysis using full Monte Carlo simulations and the measured $p_\perp$ and ϕ dependences; the techniques discussed here serve as a means to quickly extract preliminary results and as a check on the Monte Carlo simulations.

Activity	Time (hours)
Data acquisition	240
Configuration changes	100
Calibration and checkout	20
Total	**360 (15 days)**

Table 3: Beam time request for the proposed experiment

3 Summary

We request 15 days of beam in Jefferson Lab Hall C in order to perform the first experimental tests of factorization at low ν and duality in pion electroproduction, a phenomenon whose analog in the inclusive realm has been shown to hold to high precision over a large range of kinematics. Several facts indicate that we can utilize fragmentation functions to extract information about duality from pion electroproduction data, and recent Jefferson Lab test runs strongly suggest the existence of such dual behavior.

References

[Afa98] A. V. Afanasev, Physics & Instrumentation with 6-12 GeV Beams, Thomas Jefferson Laboratory Accelerator Facility, Ed. S. Dytman, H. Fenker, P. Roos, p. 263 (1998).

[Ack98] K. Ackerstaff *et al.*, Phys. Rev. Lett. **81**, 5519 (1998).

[Arn95] M. Arneodo *et al.*, Phys. Lett. B **364**, 107 (1995).

[Bin95] J. Binnewies, B. A. Kniehl, and G. Kramer, Phys. Rev. D **52**, 4947 (1995).

[Blo70] E. D. Bloom and F. J. Gilman, Phys. Rev. Lett. **25**, 1140 (1970).

[Blo71] E. D. Bloom and F. J. Gilman, Phys. Rev. D **4**, 2901 (1971).

[Car90] C. E. Carlson and N. C. Mukhopadhyay, Phys. Rev. D **41**, 2343 (1990).

[Car98] C. E. Carlson, Physics & Instrumentation with 6-12 GeV Beams, Thomas Jefferson Laboratory Accelerator Facility, Ed. S. Dytman, H. Fenker, P. Roos, p. 17 (1998).

[Cas98] C. Caso *et al.*, The European Physical Journal **C3** (1998) 1.

[Dak73] J. T. Dakin *et al.*, Phys. Rev. Lett. **31**, 786 (1973).

[DeR77a] A. De Rújula, H. Georgi, and H. D. Politzer, Phys. Lett. B **64**, 428 (1977).

[DeR77b] A. De Rújula, H. Georgi, and H. D. Politzer, Annals Phys. **103**, 315 (1977).

[Fro94] B. Frois and P. J. Mulders, Workshop on CEBAF at Higher Energies, Thomas Jefferson Laboratory Accelerator Facility, Ed. N. Isgur, P. Stoler, p. 309 (1994).

[Glu98] M. Glück, E. Reya, and A. Vogt, e-print hep-ph/9806404 (1998).

[Han63] L. N. Hand, Phys. Rev. **129**, 1834 (1963).

[Haw98] E866 Collaboration, E. A. Hawker *et al.*, Phys. Rev. Lett. **80**, 3715 (1998); E866 Collaboration, J. C. Peng *et al.*, e-print hep-ph/9804288 (1998).

[Lai97] H. L. Lai *et al.*, Phys. Rev. D **55**, 1280 (1997).

[Lig88] J. W. Lightbody, Jr. and J. S. O'Connell, Computers in Physics, Journal Section, May/June 1988.

[Mar94] A. D. Martin, R. G. Roberts, and W. J. Stirling, Phys. Rev. D **50**, 6734 (1994).

[Mar77] J. F. Martin and L. S. Osborne, Phys. Rev. Lett. **38**, 1193 (1977).

[Moh99] R. M. Mohring, dissertation, University of Maryland (unpublished) (1999).

[Nic98] I. Niculescu, dissertation, Hampton University (unpublished) (1998).

[Nic99] I. Niculescu *et al.*, two letters submitted to Phys. Rev. Lett. *Copies of these articles are attached to the proposal.*

[Slo88] T. Sloan, G. Smadja, and R. Voss, Phys. Rep. **162**, 45 (1988).

Experimental Verification of Quark-Hadron Duality

I. Niculescu,[1] C.S. Armstrong,[2] J. Arrington,[3] K.A. Assamagan,[1] O.K. Baker,[1,5] D.H. Beck,[4] C.W. Bochna,[4] R.D. Carlini,[5] J. Cha,[1] C. Cothran,[6] D.B. Day,[6] J.A. Dunne,[5] D. Dutta,[7] R. Ent,[5] B.W. Filippone,[3] V.V. Frolov,[8] H. Gao,[4] D.F. Geesaman,[9] P.L.J. Gueye,[1] W. Hinton,[1] R.J. Holt,[4] H.E. Jackson,[9] C.E. Keppel,[1,5] D.M. Koltenuk,[12] D.J. Mack,[5] D.G. Meekins,[2,5] M.A. Miller,[4] J.H. Mitchell,[5] R.M. Mohring,[10] G. Niculescu,[1] D. Potterveld,[9] J.W. Price,[8] J. Reinhold,[9] R.E. Segel,[7] P. Stoler,[8] L. Tang,[1,5] B.P. Terburg,[4] D. Van Westrum,[11] W.F. Vulcan,[5] S.A. Wood,[5] C. Yan,[5] B. Zeidman[9]

[1] *Hampton University.* [2] *College of William and Mary.* [3] *California Institute of Technology.* [4] *University of Illinois at Urbana-Champaign.* [5] *Thomas Jefferson National Accelerator Facility.* [6] *University of Virginia.* [7] *Northwestern University.* [8] *Rensselaer Polytechnic Institute.* [9] *Argonne National Laboratory.* [10] *University of Maryland.* [11] *University of Colorado at Boulder.* [12] *University of Pennsylvania.*

(December 8, 1999)

A newly-obtained sample of inclusive electron-nucleon scattering data has been analyzed for precision tests of quark-hadron duality. The data are in the nucleon resonance region, and span the range $0.3 < Q^2 < 5.0$ (GeV/c)^2. Duality is observed both in limited and extended regions around the prominent resonance enhancements. Higher twist contributions to the F_2 structure function are found to be small on average, even in the low Q^2 regime of ≈ 0.5 (GeV/c)^2. Using duality, an average scaling curve is obtained. In all cases, duality appears to be a non-trivial property of the nucleon structure function.

The interpretation of the resonance region in inclusive electron-proton scattering and its possible connection with deep inelastic scattering has been a subject of interest for nearly three decades since quark-hadron duality ideas, which successfully described hadron-hadron scattering [1], were first extended to electroproduction. Bloom and Gilman [2] showed that it was possible to equate the nucleon resonance region structure function $\nu W_2(\nu, Q^2)$ (at some typically low Q^2 value) to the structure function F_2 in the deep inelastic regime of electron-quark scattering (at some higher value of Q^2). These structure functions are obtained from inclusive electron-nucleon scattering where the substructure of the nucleon is probed with virtual photons of mass $-Q^2$ and energy ν. The resonance structure function was demonstrated to be equivalent in average to the deep inelastic one, with these averages obtained over the same range in a scaling variable $\omega' = 1 + W^2/Q^2$, where W is the invariant mass. Bloom and Gilman's quark-hadron duality qualitatively explained the data in the range $1 \leq Q^2 \leq 10$ (GeV/c)^2.

This relationship between resonance electroproduction and the scaling behavior observed in deep inelastic scattering suggests a common origin for both phenomena. Inclusive deep inelastic scattering on nucleons is a firmly-established tool for the investigation of the quark-parton model. At large enough values of W and Q^2, Quantum Chromodynamics (QCD) provides a rigorous description of the physics that generates the Q^2 behavior of the nucleon structure function $F_2 = \nu W_2$. The well-known logarithmic scaling violations in the F_2 structure function of the nucleon, predicted by asymptotic freedom, played a crucial role in establishing QCD as the accepted theory of strong interactions [3,4]. However, as Q^2 decreases, the description of the nucleon's structure cannot be expressed in terms of single parton densities with simple logarithmic behavior in Q^2. Inverse power violations in Q^2, physically representing initial and final state interactions between the struck quark and the remnants of the target (termed higher twist effects), must be taken into account as well.

An analysis of the resonance region in terms of QCD was first presented in [5,6], where Bloom and Gilman's approach was re-interpreted, and the integrals of the average scaling curves were equated to the n =2 QCD moments of the F_2 structure function. The Cornwall-Norton moments of the structure function may be expressed as $\int_0^1 x^{n-2} F_2(x) dx$ [7], where $x = Q^2/2M\nu$ is the Bjorken scaling variable, M is the nucleon mass, and n is an integer index. The moments can be expanded, according to the operator product expansion, in powers of $1/Q^2$, and the fall of the resonances along a smooth scaling curve with increasing Q^2 was explained in terms of this QCD twist expansion of the structure function. The conclusion of [5] was that changes in the lower moments of the F_2 structure function due to higher twist effects are small, so that averages of this function over a sufficient range in x at moderate and high Q^2 are approximately the same. Duality is expected to hold so long as $O(1/Q^2)$ or higher inverse power scaling violations are small.

Substantial progress has been made both theoretically in understanding QCD in the past twenty years and experimentally in determining the scaling behavior of the F_2 structure function. Combining the latter with the new precision resonance data presented here [8], it is now possible to revisit quark-hadron duality with a more quantitative approach, addressing the recent theoretical interest in the topic (see, for example, [9–15]).

The data were obtained in Hall C, using the CEBAF accelerator at Jefferson Lab (JLab). Electron beam energies between 2.4 and 4 GeV, with currents between 20 and 100 μAmps were incident on 4 and 15 ($\pm$ 0.01) cm long liquid hydrogen and deuterium targets. Scattered electrons were detected in both the High Momentum Spectrometer (HMS) and the Short Orbit Spectrometer (SOS), each utilized in a single arm mode to measure the inclusive cross sections.

Nine spectra were obtained for hydrogen and eight for deuterium, covering the invariant mass range $1.0 < W^2 < 4.0$ GeV^2, with central four-momenta in the range $0.3 \leq Q^2 \leq 5.0$ (GeV/c)^2. The structure function $F_2 = \nu W_2$ was extracted from the measured differential cross section σ, using

$$\frac{\sigma \nu Q^4}{4\alpha^2 E'^2} = F_2 \left[\cos^2(\frac{\theta}{2}) + 2\sin^2(\frac{\theta}{2}) \frac{1+\nu^2/Q^2}{R+1} \right]. \quad (1)$$

Here, α is the fine structure constant, θ is the electron scattering angle, and E' is the scattered electron energy. $R = \sigma_L/\sigma_T$ is the ratio of longitudinal to transverse cross sections. This quantity will be measured at JLab [16], but is currently unknown at the $\pm$100% level in the resonance region for $Q^2 \geq 1$ (GeV/c)^2 [17]. The possible variation of R effects a 2% systematic uncertainty in the extracted F_2 data.

Sample νW_2 spectra extracted from the measured differential cross sections from hydrogen are plotted in Fig. 1 as a function of the Nachtmann scaling variable $\xi = 2x/(1+\sqrt{1+4M^2x^2/Q^2})$. It has been shown that ξ is the correct variable to use in studying QCD scaling violations in the nucleon [18,5]. The arrows indicate $x = 1$ (elastic scattering) kinematics for the four values of Q^2 shown. The solid and dashed curves are from a parameterization [19] of deep inelastic proton structure function data at $Q^2 = 10$ and 5 (GeV/c)^2, respectively. Notice that the resonance spectra at higher (lower) Q^2 appear at higher (lower) ξ on the deep inelastic scaling curve, but that the curve generally represents an average of the data at the disparate kinematics. This is a qualitative manifestation of the original Bloom and Gilman observation.

Because the data were obtained at fixed spectrometer angles, with a few overlapping fixed central momenta, the raw spectra in missing mass (W^2) cover a range in Q^2. The spectra in Fig. 1 have been adjusted to the Q^2 value at $W^2 = 2.5$ GeV^2 for each using a global fit [17] to inclusive resonance region spectra. The difference between the raw and adjused spectra is $\approx$ 3% when integrated. The statistical uncertainty in the data is $\approx$ 1%, smaller than the symbols plotted. The overall systematic uncertainty in the cross sections due to experimental considerations such as target density, beam charge, beam energy, spectrometer acceptance, radiative corrections, detection efficiency, and the value of R, is 3% and is not depicted.

To quantify the observed duality, we show in Fig. 2 the Q^2 dependence of the integral ratio quantity I(Res/DIS), the ratio of the structure function $\nu W_2 = F_2$ obtained from the resonance data, integrated over the region from pion threshold to the onset of the deep inelastic regime ($W^2 = 4$ GeV^2), compared to the indicated deep inelastic structure functions integrated over the same region of ξ:

$$I(Res/DIS) = \frac{\int_{\xi(W^2=4.0)}^{\xi(W^2=1.1)} F_2^{data}(\xi, Q^2 = fixed) d\xi}{\int_{\xi(a)}^{\xi(b)} F_2^{scaling}(\xi, Q^2 = 10) d\xi}. \quad (2)$$

Here, $\xi(a,b)$ correspond to the same value of ξ used in the numerator integral, which at the higher Q^2 of the deep inelastic data no longer correspond to $W^2 = (4.0, 1.1)$, but to some higher $W^2 = (a,b)$. The range $1.1 \leq W^2 \leq 4.0$ GeV^2 is the resonance region of the data. In all cases but the Resonance fit (discussed below), the scaling region structure functions are integrated as a function of ξ at fixed $Q^2 = 10$ (GeV/c)^2. The higher W^2 deep inelastic data are, for the same region in ξ, at higher Q^2. The integral ratio data are plotted as a function of the fixed Q^2 values associated with the measured resonance spectra.

The uncertainties shown represent the experimental uncertainty in the numerator integral only, obtained from the correlated systematic uncertainties in the resonance data. The high Q^2 (above 4 (GeV/c)^2) numerator values are generated from a global fit to inclusive SLAC resonance region data [17] and are assigned an uncertainty representing a combination of experimental uncertainty and normalization considerations involved in utilizing the older data sets [20]. Also shown are very low Q^2 (< 0.5 (GeV/c)^2) resonance data from SLAC [21].

When used to obtain the deep inelastic denominator of the ratios in Fig. 2, the well-known CTEQ4 LQ [22] and MRS(G) LQ [19] scaling curves display a marked deviation from unity which increases with Q^2. This is not necessarily due to higher twist effects, but rather to the difficulty in accurately modeling the large ξ behavior of the structure function. With increasing Q^2, the moments are determined by a smaller and smaller region near $\xi = 1$. Unfortunately, there is a limited amount of deep inelastic F_2 data currently available at large ξ and x and these curves fall below both the average resonance data and the NMC parameterization above $\xi \gtrsim 0.7$.

The points on Fig. 2 labeled NMC represent ratios obtained using a parameterization of lower x deep inelastic F_2 data from CERN [23], which links smoothly to a global fit [20] to higher x deep inelastic data from SLAC, in the denominator integral. Because this is a fit to the data, it may implicitly contain higher twist effects. Using the NMC parameterization, the ratio (Res/DIS) is above unity, but constant at about 1.2. The ratio decreases to about 1.1 when the appropriate logarithmic Q^2 dependence is included to obtain the parameterization at $Q^2 = 5$ (GeV/c)^2. This effect is indicated by the dashed line in the figure.

To obtain the points labeled Resonance fit in Fig. 2, a fit to the *average* strength of *all* the hydrogen resonance spectra was obtained and utilized as a scaling curve. This approach assumes duality, and therefore that the average of the resonance data is equivalent to a proper scaling curve. For small bins in ξ, resonance νW_2 data were averaged, regardless of Q^2, W^2. These average points were then fit as a function of ξ only, and the resultant scaling curve was obtained using a form similar to the x-dependent part of the NMC parameterization [23]. The scaling curve denoted Resonance fit is, then:

$$F_2 = \xi^{0.8699}(1-\xi)^{1.4832}\,[0.2083 - 2.9816(1-\xi) + 17.1260(1-\xi)^2 - 24.1150(1-\xi)^3 + 12.3640(1-\xi)^4]\,. \quad (3)$$

To constrain the fit in the kinematic regions beyond the scope of the data, data obtained from [21] were also used below $Q^2 = 0.5$ (GeV/c)^2 and $\xi = 0.2$. Resonance data in the range $5 < Q^2 < 8$ (GeV/c)^2 were generated from [17] and used to constrain the fit at large ξ. Note that the ratio I(Res/DIS) in Fig. 2 comparing the resonance strength to the Resonance fit scaling curve need not be unity here even though the curve was extracted from the resonance data. The average scaling curve strength at any given value of ξ was obtained from a kinematic range of data at variant values of W^2 and Q^2 oscillating around this curve. The individual spectra used to obtain the plotted ratios are, however, at the indicated fixed Q^2 values only.

The total integrated strength in the region below $W^2 = 4$ GeV^2 averages to values within 10% of the Resonance scaling curve integrated over the same region in ξ, even at Q^2 values as low as ≈ 0.5. Similarly, the ratio I(Res/DIS) is a constant ≈ 1.2, within 10%, when the NMC deep inelastic parameterization is utilized. Additionally, it is indicated that this latter ratio would tend toward unity if it were possible to compare the resonance region data with lower Q^2 values of the deep inelastic. In the QCD-based explanation of duality (e.g. [5]), these results indicate that higher twist effects are surprisingly reduced if the data are integrated over this *full* region. A more stringent test of this reduction of higher twist effects may be found in an analysis of higher order moments due to the greater contribution, at higher n, of larger x, ξ data. In a duality representation, this motivates the need for precision resonance region measurements at higher Q^2 - data which are planned but not yet available [24].

Fig. 3 shows the same duality integral ratio as in Fig. 2, but here obtained more locally, in restricted ξ ranges around the three prominent resonance enhancement regions observed in inclusive nucleon resonance electroproduction, i.e. around the masses of the Δ $P_{33}(1232)$ ($1.3 \le W^2 \le 1.9$ GeV^2), the $S_{11}(1535)$ ($1.9 \le W^2 \le 2.5$ GeV^2), and the $F_{15}(1680)$ ($2.5 \le W^2 \le 3.1$ GeV^2) resonances, and in the higher W^2 region above these ($3.1 \le W^2 \le 3.9$ GeV^2). The uncertainties shown were computed as in Fig. 2. The latter higher mass ratios, which compare near deep inelastic data to deep inelastic data are essentially one and similar to the results in Fig. 2. It has been pointed out [25] that the Δ resonance form factor decreases faster in Q^2 than the leading order perturbative QCD Q^{-4} behavior which the scaling curve should reflect. A similar observation may be made from Fig. 3 where the ratio (Res/DIS) drops below unity in the region $1 < Q^2 < 3.5$ (GeV/c)^2. The S_{11}, on the other hand, appears systematically higher than the others. Generally, however, the lower mass resonances appear to average to the deep inelastic strength, manifesting duality behavior even in these limited ranges of ξ at low Q^2 where higher twist effects might be expected to be large.

By utilizing new inclusive data in the resonance region at large x, it has been possible to revisit quark-hadron duality experimentally for the first time in nearly three decades. These new data, combined with the extensive global measurements of the F_2 structure function from deep inelastic scattering, allow for precision tests of duality in electron-nucleon scattering. The original duality observations are verified, and the QCD moment explanation indicates that higher twist contributions to the $n = 2$ moment of the F_2 structure function are small or cancelling, even in the low Q^2 regime of $Q^2 \approx 0.5$ (GeV/c)^2. Duality is observed to hold for local resonance enhancements individually, as well for the entire $1 \le W^2 \le 4$ GeV^2 resonance region. In all cases, duality appears to be a non-trivial dynamic property of the nucleon structure function.

We acknowledge the outstanding work of the staff of the accelerator division at the Thomas Jefferson National Accelerator Facility. C.E.K. and R.E. wish to thank A. Radyushkin for many useful discussions. This work is supported in part by research grants from the U.S. Department of Energy and the National Science Foundation.

[1] P.D.B. Collins, *An Introduction to Regge Theory and High Energy Physics* (Cambridge University Press, Cambridge, 1977)
[2] E.D. Bloom and F.J. Gilman, Phys. Rev. D **4** (1970) 2901
[3] G. Altarelli, Phys. Rep. **81** (1982) 1
[4] A.J. Buras, Rev. Mod. Phys. **52** (1980) 199
[5] A. De Rujula, H. Georgi, and H.D. Politzer, Ann. Phys. **103** (1977) 315
[6] H. Georgi and H.D. Politzer, Phys. Rev. D **14** (1976) 1829
[7] R. Roberts, *The Structure of the Proton* (Cambridge University Press, Cambridge, 1990)

[8] I. Niculescu, Ph.D. Thesis, Hampton University, 1999
[9] X. Ji and P. Unrau, Phys. Rev. D **52** (1995) 73
[10] V.M. Belyaev and A. Radyushkin, Phys. Lett. B **350** (1995) 194
[11] G. West, hep-ph/9612403 (1996)
[12] G. Ricco *et al.*, Phys. Rev. C **57** (1998) 356
[13] C. Coriano, H-N. Li, and C. Savkli, J. High En. Phys. 9807 (1998) 008
[14] C. Carlson and N. Mukhopadhyay, Phys. Rev. Lett. **74** (1995) 1288
[15] M. Anghinolfi *et al.*, Nucl. Phys. **A602** (1996) 405
[16] Jefferson Lab Experiment E94-110
[17] C. Keppel, Proceedings of the Workshop on CEBAF at Higher Energies, Eds. N. Isgur and P. Stoler (1994) 237
[18] O. Nachtmann, Nucl. Phys. **B63** (1975) 237
[19] A.D. Martin, R.G. Roberts, and W.J. Stirling, Phys. Rev. D **50** (1994) 6734
[20] L.W. Whitlow *et al.*, Phys. Lett. **B282** (1992) 475
[21] S. Stein *et al.*, Phys. Rev. D **12** (1975) 1884
[22] H.L. Lai *et al.*, Phys. Rev. D **55** (1997) 1280
[23] M. Arneodo *et al.*, Phys. Lett. **B364** (1995) 107 (1984) 295
[24] Jefferson Lab Experiment E97-010
[25] P. Stoler, Phys. Rev. Lett. **66** (1991) 1003

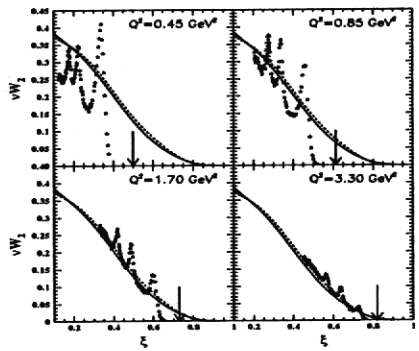

FIG. 1. Sample hydrogen νW_2 structure function spectra obtained at $Q^2 = 0.45, 0.85, 1.70$, and 3.30 (GeV/c)^2 and plotted as a function of the Nachtmann scaling variable ξ. Arrows indicate elastic kinematics. The solid (dashed) line represents the NMC fit [23] of deep inelastic structure function data at $Q^2 = 10$ (GeV/c)^2 ($Q^2 = 5$ (GeV/c)^2).

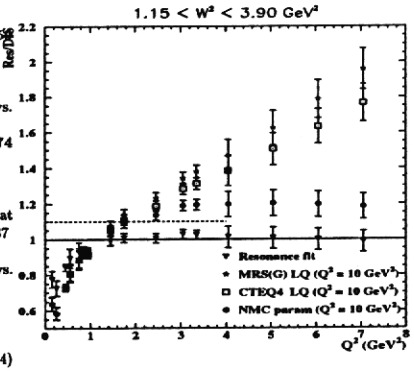

FIG. 2. The ratios of integrals obtained over the hydrogen resonance structure function in the ξ range corresponding to invariant masses between $1.1 < W^2 < 4.0$ GeV^2 (Res) to integrals of the deep inelastic structure functions obtained from parameterizations (stars are Resonance fit; circles are NMC at $Q^2 = 10$ (GeV/c)^2; squares are CTEQ4 low Q^2; triangles are MRS(G) low Q^2) for the same range in ξ (DIS). The dashed line indicates what this ratio would be if the NMC curve were obtained at $Q^2 = 5$ (GeV/c)^2.

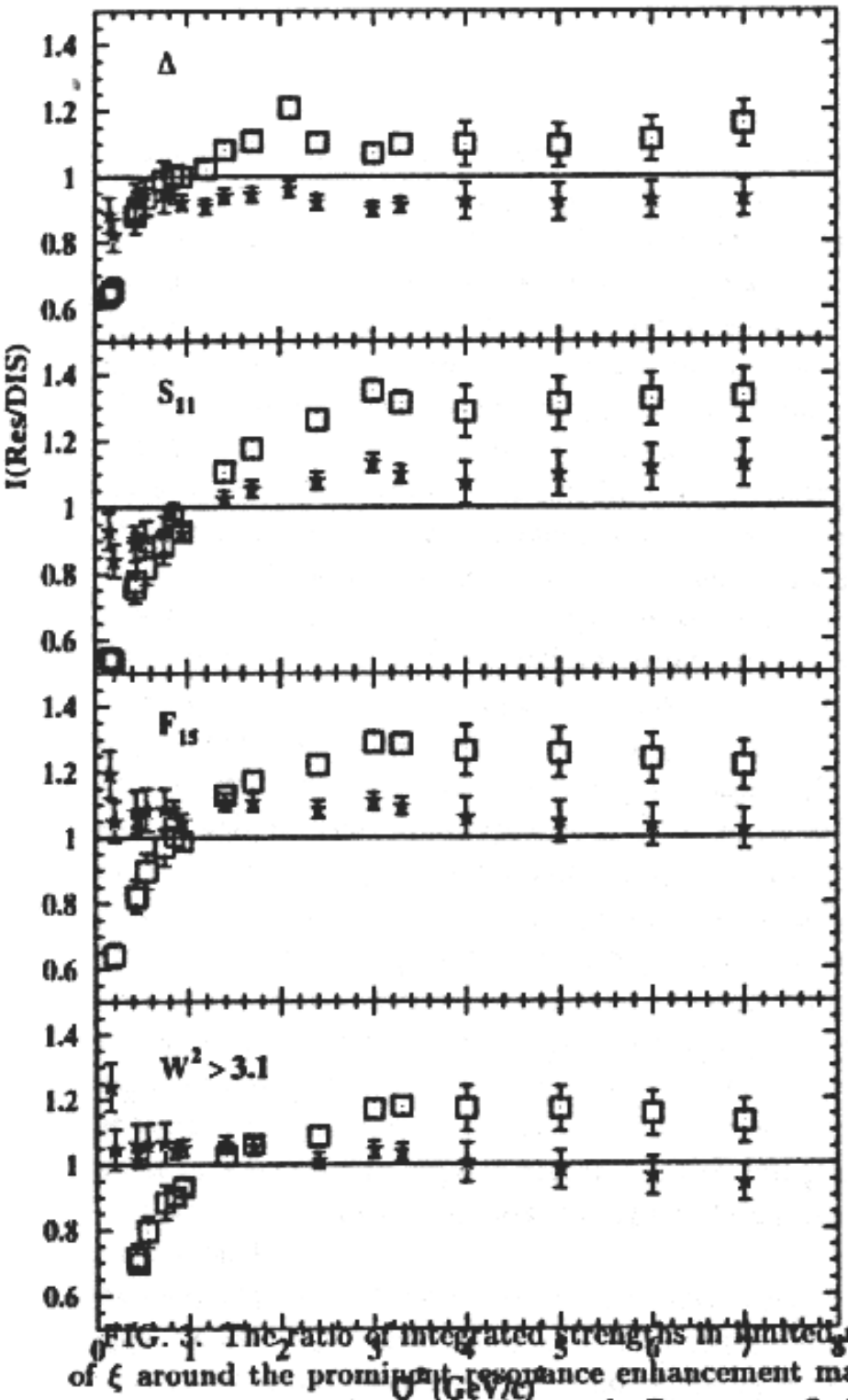

FIG. 3. The ratio of integrated strengths in limited ranges of ξ around the prominent resonance enhancement mass regions, to the strengths obtained from the Resonance fit (stars) and NMC (squares) scaling curves integrated over the same limited ξ regions.

Evidence for Valence-Like Quark-Hadron Duality.

I. Niculescu,[1] C.S. Armstrong,[2] J. Arrington,[3] K.A. Assamagan,[1] O.K. Baker,[1,5] D.H. Beck,[4] C.W. Bochna,[4] R.D. Carlini,[5] J. Cha,[1] C. Cothran,[6] D.B. Day,[6] J.A. Dunne,[5] D. Dutta,[7] R. Ent,[5] V.V. Frolov,[8] H. Gao,[4] D.F. Geesaman,[9] P.L.J. Gueye,[1] W. Hinton,[1] R.J. Holt,[4] H.E. Jackson,[9] C.E. Keppel,[1,5] D.M. Koltenuk,[12] D.J. Mack,[5] D.G. Meekins,[2,5] M.A. Miller,[4] J.H. Mitchell,[5] R.M. Mohring,[10] G. Niculescu,[1] D. Potterveld,[9] J.W. Price,[8] J. Reinhold,[9] R.E. Segel,[7] P. Stoler,[8] L. Tang,[1,5] B.P. Terburg,[4] D. Van Westrum,[11] W.F. Vulcan,[5] S.A. Wood,[5] C. Yan,[5] B. Zeidman[9]

[1] *Hampton University.* [2] *College of William and Mary.* [3] *California Institute of Technology.* [4] *University of Illinois at Urbana-Champaign.* [5] *Thomas Jefferson National Accelerator Facility.* [6] *University of Virginia.* [7] *Northwestern University.* [8] *Rensselaer Polytechnic Institute.* [9] *Argonne National Laboratory.* [10] *University of Maryland.* [11] *University of Colorado at Boulder.* [12] *University of Pennsylvania.*

(December 1, 1999)

A newly obtained data sample of inclusive electron-nucleon scattering from both hydrogen and deuterium targets is analyzed. These JLab data are in the nucleon resonance region up to four-momentum transfers of 5 (GeV/c)^2. The data are in agreement with SLAC data at similar kinematics, and are found to follow an average scaling curve. The inclusion of low-momentum transfer data yields a scaling curve resembling deep inelastic neutrino-nucleus scattering data, suggesting a sensitivity to valence-like structure only.

Nearly thirty years ago Bloom and Gilman observed that the electroproduction of resonances resembles the scaling behavior of the deep inelastic structure function, if expressed in terms of a scaling variable connecting the two different kinematic regions, and if averaged over a large range of invariant mass W [1]. It was suggested that this relationship between resonance electroproduction and the scaling behavior observed in deep inelastic scattering hinted at a common origin for both phenomena, called local duality. A quantitative Quantum Chromodynamics (QCD) analysis of this empirical observation was given by De Rujula, Georgi, and Politzer [2]. They showed that the resonances oscillate around an *average* scaling curve. Although electroproduction of resonances is a strongly non-perturbative phenomenenon, the resonance strengths average to a global scaling curve, resembling the deep inelastic scaling curve, as the higher-twist effects are not large, if averaged over a large kinematic region.

Higher-twist effects can be viewed as processes where the struck quark communicates with one or more of the spectator quarks by gluon exchange. In the deep inelastic F_2 data, higher-twist terms have been found to be small for Bjorken $x < 0.40$ [3], and insignificant for $x \approx 0.01$, even at $Q^2 \simeq 1$ (GeV/c)^2, where Q is the four-momentum transfer [4,5]. On the other hand, gauge invariance requires F_2 to vanish linearly with Q^2 at $Q^2 = 0$ (GeV/c)^2 [6], suggesting non-perturbative effects govern this region. In this Letter we assume higher-twist effects, if averaged over the full resonance region, to be small, even at relatively low momentum transfers, and thus local duality to remain valid. A quantitative verification of this assumption will be presented elsewhere [7].

A sample of high-precision data in the nucleon resonance region, in combination with substantial progress made over the last twenty years in determining the scaling behavior of deep inelastic structure functions with electron, muon, and neutrino probes, enables us to revisit local duality in detail. We investigate the connection between resonance electroproduction and deep inelastic scattering to lower four-momentum transfers than previously investigated, and consider possible implications.

We accumulated data in the nucleon resonance region, $1 < W^2 < 4$ (GeV/c)^2, for both hydrogen and deuterium targets [8]. Measurements in the elastic region were included in the data to verify our absolute normalizations to better than 2%. The data were obtained in Hall C at Jefferson Lab (JLab), using electron beam energies between 2.4 and 4 GeV. Incident beam currents between 20 and 100 μA were used on 4 and 15 cm long targets. Scattered electrons were detected in both the High Momentum Spectrometer (HMS) and the Short Orbit Spectrometer (SOS) [8], each utilized in a single arm mode to measure the inclusive cross sections. At all beam energy-scattering angle combinations, the central momentum of the spectrometers was varied to cover the full resonance region. The change in central momentum was kept smaller than the momentum acceptance of each spectrometer, to ensure that overlapping data were accumulated. The internal consistency of the data, within a 16% momentum acceptance for HMS and a 30% momentum acceptance for SOS, was found to be always better than 3%. The Q^2 range covered by our data set is between 0.3 and 5 (GeV/c)^2. We accumulated of order 10^5 counts for every beam energy-scattering angle combination (9 in total for hydrogen, 8 for deuterium). In all cases, the overall systematic uncertainty in the measured cross sections due to target density, beam charge, beam energy, spectrometer acceptance, radiative corrections,

and detection efficiency is less than 3% and larger than the statistical uncertainties [8–10].

We extracted the structure function F_2 from the measured differential cross sections $\sigma = \frac{d^2\sigma}{d\Omega dE'}$ like $F_2 \sim \sigma \times (1+R)/(1+\epsilon R)$ [11]. Here ϵ is the virtual-photon polarization and R is the ratio of longitudinal to transverse cross sections. We used a value of $R = 0.2$ for the present analysis, but the results are consistent within 2% if a parametrization of this quantity based on deep inelastic scattering data at moderate Q^2 is utilized [12]. However, we note that this quantity is presently only known at the $\pm$100% level in the nucleon resonance region above $Q^2 \approx 1$ (GeV/c)^2.

A sample of the extracted F_2 data in the nucleon resonance region are shown in Fig. 1a for the hydrogen target, and in Fig. 1b for the deuterium target, as functions of the Nachtmann scaling variable ξ. These figures also include some low Q^2 data from SLAC [13,14]. In terms of the Nachtmann variable $\xi = 2x/(1+\sqrt{1+4M^2x^2/Q^2})$ [15], where M is the nucleon mass, a pattern of scaling violations has been formulated within a QCD framework [2]. The variable ξ takes target-mass corrections into account, necessary as the quarks can not be treated as massless partons for low to moderate momentum transfers. Note that, for low x or large Q^2, the scaling variable ξ is almost identical to the Bjorken scaling variable x.

It is clear from Fig. 1 that indeed the data oscillate around a global curve. This reiterates the well-known local duality picture; the data at various values of Q^2 and W^2 average to a smooth curve if expressed in terms of ξ. For comparison, the solid curve shown represents a global fit to the wold's deep inelastic data [16] for a fixed $Q^2 =$ 10 (GeV/c)^2 (NMC10, solid). Previous analyses of local duality have concentrated on a comparison of such deep inelastic constrained curves with nucleon resonance data for $Q^2 \geq 1$ (GeV/c)^2, corresponding to a lower cutoff of $\xi \approx 0.3$. However, as one can see from Fig. 1, the resonance data still seem to oscillate around a global curve, even in the region $\xi \leq 0.3$. This suggests that also in this region the effect of the higher-twist terms is reduced if *averaged* over the full resonance region - consistent with the earlier QCD analysis of the $\xi > 0.3$ region [2]. Note that, for sake of visual clarity, we could not include all of the existing spectra.

From now on we will concentrate on the region of $\xi \leq 0.3$. We initially construct a scaling curve representing the average of the resonance data in the region $M^2 \leq W^2 < 4$ (GeV/c)^2, for $Q^2 < 5$ (GeV/c)^2. The average curve for the hydrogen data is shown as a shaded band in Figure 2, where the width of the band takes the systematic uncertainties of the procedure into account. Note that the scaling curve at some ξ value will represent the average of proton resonance data for an extended (W^2, Q^2)-region, but that the average Q^2 will globally increase with ξ. The curves shown represent the global fit to the world's deep inelastic data [16] for a fixed $Q^2 =$ 10 (GeV/c)^2 (NMC10, solid), and for a fixed $Q^2 = 2$ (GeV/c)^2 (NMC2, dashed). Whereas the difference between the NMC fit for fixed $Q^2 = 10$ (GeV/c)^2 and $Q^2 = 2$ (GeV/c)^2 is small, and expected from logarithmic scaling violations, the difference between these NMC fits and our data (with $Q^2 \approx 0.3$ (GeV/c)^2) derived from the duality-averaged scaling curve is dramatic at low ξ.

We have used the next-to-leading order calculations of Glück, Reya and Vogt (GRV) [17] to investigate this in more detail. We use the GRV calculations since these are the only ones enabling us to evolute F_2 down to the low momentum transfers of our measurements. In the GRV model, the shape of the gluon and quark-antiquark sea seen by experiment is dynamically generated through gluon bremsstrahlung. The GRV input distribution has been fixed by assuming only valence and valence-like (the input sea quark and gluon distributions also approach zero as $x \to 0$) quark distributions at a finite Q^2 value, constrained with appropriate Q^2-evolutions to deep inelastic F_2 data. We display in Fig. 2 the results of the calculations (GRV, dot-dashed), for Q^2 values close to the average Q^2 of our scaling curve. To compare with the very lowest ξ-region of our data, we also show the *input* distribution itself at $Q^2 = 0.40$ (GeV/c)^2. Note that we here compare data and GRV calculations in a region not advocated by the authors, as "in the very low Q^2 region below 1 (GeV/c)^2 non-perturbative higher-twist contributions are expected to become relevant" [18]. However, as mentioned, our assumption is that the higher-twist effects are reduced, if averaged over the full resonance region. The dotted curve in Fig. 2 denotes the GRV input distribution reflecting *only* the valence quark distributions (i.e. there are no sea quark contributions at all). One can verify that this input distribution is even closer to the actual nucleon-resonance averaged data, at similar Q^2, than the similar input distribution including valence-like effects (dot-dashed curve). The similarity of the various calculations, starting with the mentioned input distributions of Ref. [17], and the average scaling curve given by the nucleon resonance data, suggests that the duality-averaged scaling curve is dominated by valence-quark or valence-like quark contributions.

To verify this, we show in Fig. 3 a comparison of the averaged scaling curve from the deuterium resonance data (solid curve) with a selection of the world's data for the xF_3 structure function. The xF_3 structure function can be accessed by deep inelastic neutrino-iron scattering [19,20], and is associated with the parity-violating term in the hadronic current. Thus, xF_3 measures in the quark-parton model the difference between quark and anti-quark distributions, and is to first order insensitive to sea quark distributions. To enable a direct comparison, we have multiplied our average scaling curve by a factor of 18/5 to account for the quark charges, and have applied a straightforward nuclear correction to the xF_3 data to obtain neutrino-deuterium data [21]. Although